J Intell Robot Syst (2018) 90:269–286
https://doi.org/10.1007/s10846-017-0658-7

Optimal Control of Screw In-pipe Inspection Robot with Controllable Pitch Rate

H. Tourajizadeh[1] · M. Rezaei[1] · A. H. Sedigh[1]

Received: 5 June 2016 / Accepted: 8 June 2017 / Published online: 27 September 2017

Abstract A Steerable in-pipe inspection robot is designed in this paper and its optimal control based on linear quadratic regulator (LQR) approach is performed subject to input minimization. In-pipe inspection robots are necessary mobile robots in order to investigate the pipelines. Most of the in-pipe inspection robots are limited to move with a constant pitch rate. An in pipe inspection robot is proposed in this paper which is based on screw locomotion and its steering angle is also controllable in order to handle the pitch rate of the movement and bypass the probable obstacles. Since the proposed robot is multivariable with more than one controlling input, minimizing its control inputs are extremely useful. The goal of this paper is to extract the dynamic model of the mentioned steerable screw in-pipe inspection robot and controlling it within a predefined trajectory in an optimal way. The proper mechanism is designed and its related kinematics and kinetics are derived. Afterwards the objective function is defined based on minimizing the controlling input and maximizing the accuracy of movement. The nonlinear state space is linearized around its operating point and optimization is implemented using Linear Quadratic Regulator (LQR). The efficiency of the designed robot and controller and the optimality of its controlling procedure are investigated by the aid of MATLAB simulation and comparative analysis. It is proved that the designed robot is able to move with controllable pitch rate and acceptable accuracy while the obstacles can be avoided and the energy consumption is optimized. At the end the validity of modeling and simulation in MATLAB is also verified by modeling the robot in ADAMS and comparing the results.

Keywords In-pipe inspection robot · Variable pitch rate · Obstacle avoidance · Optimal control · LQR

1 Introduction

Mobile Robots are nowadays extremely important in industries in order to manage investigations, repairs, manipulations and other functions. In recent years, a significant volume of researches has been focused on improvement of the mobile robots and lots of approaches are proposed for tracking and controlling of these kinds of robots. Peng et al. [1] investigated the adaptive distributed formation control problem for multiple non-holonomic wheeled mobile robots. Scaglia et al. [2] studied the problem of mobile robots under uncertainties. Although the mobility of these kind of robots is high and their ability to do a variety of tasks is increased, however these kinds of robots are not appropriate for moving through the pipe lines since they cannot remain stable in the pipes especially during steering periods. So researchers have promoted the design of the mobile robots in order to increase their ability to move through the pipes and investigate the lines.

The new generation of robots are more suitable in order to investigate the internal space of the pipes and detect the cracks, leaks, and implement on destructive tests on them. These kinds of robots are called In-Pipe Inspection

✉ H. Tourajizadeh
tourajizadeh@khu.ac.ir

M. Rezaei
rezaee.91.m@gmail.com

A. H. Sedigh
amirhosseinseddigh@gmail.com

[1] Mechanical Engineering Department, Faculty of Engineering, Kharazmi University, Tehran, Iran

Robots(IPIRs) and they are divided into three categories. 1) Without wheel robots. 2) Caterpillar robots. 3) Wheeled robots and all of these groups are also divided into some subgroups. Numerous types of in pipe robots have been designed so far. Takahashi et al. [3] designed a robot based on earthworm motion that is composed of three locomotive units. Zagler and Pfeiffer [4] designed a leg type robot (MORITZ) which could climb through pipes with different rate of inclinations. These kinds of robots were too slow, so new generation of these robots were developed with wheel and caterpillar. Kim et al. [5] designed a caterpillar robot (wall pressed type) to provide a good friction force between the robot and pipes. This robot is able to climb through vertical pipes as a result of its wall pressed mechanism. Recently, variety types of caterpillar in-pipe inspection robots are designed. Harish and Venkateswarlu [6] designed a robot with caterpillar wheels which consists a CMOS camera, an accelerometer, a temperature sensor and a ZigBee module. Also the kinematics of the robot is considered in this paper. Caterpillar robots provides stronger propulsion friction compared to wheeled based ones. Suzumori et al. [7] developed a micro inspection robot for an in pipes robot equipped by a high-quality micro charge-coupled device (CCD) camera and a dual hand for manipulating small objects in the pipes. Despite of good maneuverability of caterpillar robots as a result of their acceptable rate of friction, their stability and adaptability respect to different pipeline geometrical shapes is not good. Wheeled based in pipe robots seems to be better solution to deal with the mentioned challenge. Zhang and Yan [8] designed a wheeled robot with active pipe-diameter adaptability. They modeled the system and extracted the differential equations. Afterward, the robot is controlled using PD and PID controllers. Roh and Choi [9] proposed a wheeled wall press in-pipe robot with a miniature differential-drive. The mechanism of differential-drive is designed considering steer ability to increase the adaptability of the robot with any pipeline configurations. Wheeled robots with wall press mechanism are so useful to increase the adaptability of the robot respect to the pipe shape, but screw drive mechanism of locomotion [10] provides a more optimal mechanism with lower cost and equipment for practical applications. Shugen Ma et al. [11] designed a multifunction in-pipe inspection robot equipped with one driving motor that is the main body of Multifunctional Mobile Unit (MMU[1]) that performs inspection tasks. They developed three kinds of MMU by installing different assemblies on the proposed versatile platform. Kakogawa and Ma [12] presented motion analysis of an in-pipe robot with screw drive mechanism. Yanheng et al. [13] proposed a flexible steering mechanism in order to move through the branches of the pipes. Although they investigated the curvature shape and direct pipes in this paper, however dynamics of the system is not extracted. In order to cancel the destructive effect of external disturbances and parametric uncertainties, it is also necessary to equip the designed robots with an active control.

Investigations about controlling the in-pipe inspection robots are so limited. Most controlling researchers have focused on mobile robots. Pyrkin et al. [14] introduced "consecutive compensator" control approach and an example of mobile robot with computer vision is considered here in order to indicate the efficiency of the proposed approach. Pitangaet al. [15] presented a new synthesis methodology based on model predictive control (MPC) which is applied to a three-wheeled omnidirectional mobile robot seeking to follow pre-established trajectories. In the field of in-pipe robots, Amir H.Heidariet al. [16] designed and developed a screw robot for inspection of in pipe lines in presence of fluid. They extracted the differential equation of the system. Afterwards the robot is controlled with fuzzy-logic based control strategy. Hao-jie Zhang et al. [17] proposed an iterative linear quadratic regulator (ILQR) method for trajectory tracking control of a wheeled mobile robot system. The proposed scheme involves a kinematic model of linearization technique, a global trajectory generation algorithm and trajectory tracking controller design. H. Lang [18] also used LQR optimizer tool for the mobile robots. All of the mentioned screw based inspection robots have a constant pitch rate which can be promoted by adding the possibility of obstacle avoidance using a steerable angle.

According to the literature, it can be seen that no research is devoted to an in-pipe inspection robot of type screw motion by which the pitch rate could be controlled by the aid of steerable wheels. The robot which is proposed in this paper is a screw in-pipe inspection robot equipped by in wheels that converts a screw motion to linear one and its pitch rate is controllable. Based on the delivered literature of the paper, the obstacle avoidance procedure of in-pipe inspection robots is either ignored in previous proposed models or this importance is done passively and by changing the path of the robot. The disadvantage of this traditional remedy is that the obstacle cannot be by-passed locally and in an online way. Also a significant controlling effort was required in previous researches to change the path and realize this obstacle avoidance while in the proposed model of screw in-pipe robot the obstacle avoidance can be realized without changing the planned path and in an online way with the least amount of energy consumption just by changing the pitch rate of the robot. Secondly according to the existing literatures about the in-pipe robots, no optimization is implemented in controlling procedure of previously delivered in-pipe robots. In this paper the closed loop control of the proposed in-pipe robot is modified by the aid of a strong optimization tool of LQR by which not only the accuracy of

[1]Multifunctional Mobile Units

tracking is satisfied but also the required controlling effort is minimized using the least amount of calculation which is suitable for online and real time applications.

To meet the mentioned goal, a novel steerable in-pipe robot is designed and its related kinematics and dynamics are extended. Afterwards, in order to control the robot in an optimal way, so the state space of the system is linearized around its operating point and the related states are controlled using LQR approach. The considered objective function is a compromise between accuracy and energy consumption. In the next section the kinematics and dynamics of the new proposed in-pipe robot is developed. Afterward in section three the optimal control scheme is presented. In order to verify the efficiency of the proposed robot and also checking the accuracy and optimality of the designed controller, some simulation studies are provided in section four using MATLAB software. The validity of the mentioned claims is proved by the aid of some comparative and analytic simulation scenarios. It is shown that by the aid of the proposed system and its related optimal controller, it is possible to control the robot through the pipelines with a controllable pitch rate, good accuracy and minimum amount of consumed energy. All of the kinematic and kinetic simulations are verified finally by modeling the robot in ADAMS and comparing the related profiles. The good agreement between the mentioned results shows the correctness of modeling and simulation of the robot in MATLAB and proves the related efficiencies.

2 Kinematics and Dynamics Modeling

2.1 Kinematics

In order to control the proposed in-pipe robot, it is first required to model the system and extract the related kinematic and kinetic formulations. In the previous researches the system was modeled with just one input as the propulsion force and two states [19]. In this paper in order to provide the obstacle avoidance ability by the aid of its variable pitch rate, one extra input is considered as the steering angle of the wheels. Thus, the first input is the torque of the main motor which provides the propulsion force and the second input is the torque of the motor which controls the steering angle of the robot. R indicates the length between the center of the robot and the internal wall of the pipe. Figure 1 indicates a simple scheme of the proposed in-pipe inspection robot.

Here by the aid of rotation of the rotor section, the stator will have a translational movement through the pipe. It can be seen from Fig. 2 that b is the length between the center of the robot and the center of the wheel, r is radius of the wheels and it can be easily shown that $R = (r + b)$. $\emptyset$ is the angle of the hull, θ is the angle of the rotation of the wheels and α is the inclined angel of the wheels.

The front wheel of the proposed system is steerable using active actuator in contrast with the one which is introduced in [19]. So the angle of the front wheel ($\boldsymbol{\alpha}$) is variable. Thus just using the proposed active steerable wheel can help us to have variable pitch rate and provide the capability of obstacle avoidance. Thus the new proposed system has two degrees of freedom which should be controlled using a multivariable controller with four states

First of all, a translation matrix is required as $\mathbf{T_z}$ in Eq. 1 that translates the local frame attached to the robot to the global reference frame attached to the ground. If we consider vector o=[0,0,0,1] which indicates the coordinate of the robot frame at t=0, the vector position of the center of the robot can be extracted respect to the angle of hull ($\emptyset$). The last element of this vector should be considered to provide the required dimensional consistency for the matrix multiplication. So the coordinate of the robot will be as $\boldsymbol{H_s}$ which is shown in Eq. 2.

$$T_z = \begin{bmatrix} 1 & 0 & 0 & 0 \\ 0 & 1 & 0 & 0 \\ 0 & 0 & 1 & R\phi\tan(\alpha) \\ 0 & 0 & 0 & 1 \end{bmatrix} \tag{1}$$

$$H_s = T_z o = \begin{bmatrix} 0 \\ 0 \\ R\phi\tan(\alpha) \\ 1 \end{bmatrix} \tag{2}$$

Considering $\dot{x}.\dot{y}.\dot{z}$ and $\dot{\emptyset}$ as the work space parameters and $\dot{\alpha}$ and $\dot{\emptyset}$ as the joint space parameters the Jacobian matrix in straight pipes can be presented as Eq. 3:

$$\begin{Bmatrix} \dot{x} \\ \dot{y} \\ \dot{z} \\ \dot{\phi} \end{Bmatrix} = \begin{bmatrix} 0 & 0 \\ 0 & 0 \\ 0 & R\tan(\alpha) \\ 0 & 1 \end{bmatrix} \begin{Bmatrix} \dot{\alpha} \\ \dot{\phi} \end{Bmatrix} \tag{3}$$

2.2 Dynamics

Dynamics of the proposed in-pipe robot is extracted in this paper as two coupled differential equations relevant to generalized coordinates (α and $\emptyset$). The equations of the system are derived by the Lagrangian approach. Related Lagrangian function is as Eq. 4:

$$L = T - V \tag{4}$$

where T and V denote the *kinetic energy* and *potential energy* due to gravitational forces, respectively. The total kinetic energy will be as Eq. 5:

$$T = T_{motor} + T_{Hull} + \Gamma(T_{w1} + T_{w2}) \tag{5}$$

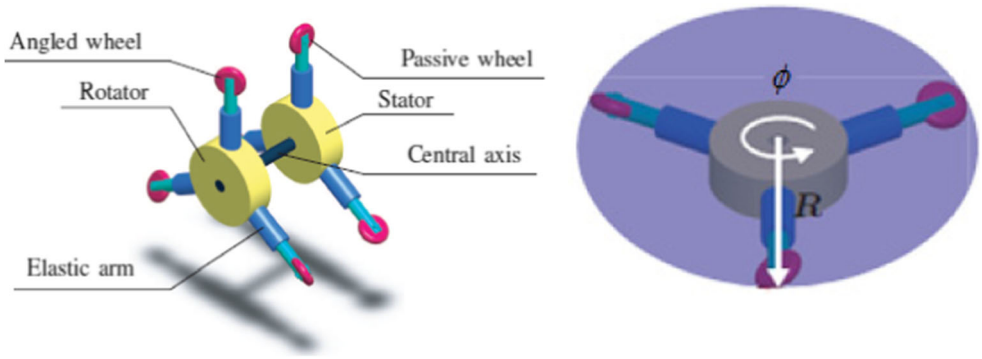

Fig. 1 An in-pipe screw robot [19]

where T_{motor}, T_{Hull}, T_{w1} and T_{w2} show kinetic energy of the motor, hull, wheels around the pipe axis and wheels around legs, respectively. Γdenotes the number of steering wheels. In Eq. 5 the kinetic energy of the passive straight wheels is ignored. The parameters of Eq. 5 are defined in Eq. 6.

$$\begin{aligned} T_{motor} &= \frac{1}{2}M_m\dot{z}^2 \\ T_{Hull} &= \frac{1}{2}M_h\dot{z}^2 + I_B\dot{\phi}^2 \\ T_{w1} &= \frac{1}{2}\left\{(mr^2+I_{WZ})\left(\frac{bC_\alpha}{b+r}\right)^2+(mr^2+I_{WX})S_\alpha^2\right\}\dot{\phi}^2 \\ T_{w2} &= \frac{1}{2}\Gamma I_{wheel}\dot{\alpha}^2 \end{aligned} \tag{6}$$

In Eq. 6 C_α and S_α denote cos (α) and sin(α), I_{wz}, I_{wx} are the wheel moment of inertia around the coordinate attached to the pipe along z and x axis respectively. Also, I_{wheel} and I_B are the wheel moment of inertia around the leg and polar moment of inertia of the hull respectively Also M_m, M_h and m are the mass of the motor, mass of the hull and mass of the wheel respectively. So according to Eq. 6 total kinetic energy can be calculated as Eq. 7.

$$\begin{aligned} T = &\frac{1}{2}\left\{\left((b+r)\frac{S_\alpha}{C_\alpha}\right)^2\alpha_M + \Gamma b^2\alpha_m + I_B\right\}\dot{\phi}^2 \\ &+\frac{1}{2}\Gamma I_{wheel}\dot{\alpha}^2 \end{aligned} \tag{7}$$

where

$$\begin{aligned} \alpha_M &= \left(M_m + M_h + \Gamma m + \Gamma\frac{I_{WX}}{r^2}\right) \\ \alpha_m &= \left(m + \frac{I_{WZ}}{r^2}\right) \end{aligned} \tag{8}$$

Moreover, an infinitesimal change in the potential energy of the robot due to the gravity during the motion along the vertical pipes can be calculated as:

$$dV = (M_m + M_h + \Gamma m)(b+r)gd\phi\tan(\alpha) \tag{9}$$

Now considering the angle of rotation of the hull (Ø) and the variation of the wheels' angle (α) as the generalized coordinates, the corresponding Lagrangian equation can be written as:

$$\frac{d}{dt}\left(\frac{\partial L}{\partial\dot{q}_i}\right) - \frac{\partial L}{\partial q_i} = Q_i \tag{10}$$

where Q_i are generalized forces which can be identified as Eq. 11 for the present work:

$$\begin{aligned} Q_1 &= T_m - T_f \\ Q_2 &= T_s \end{aligned} \tag{11}$$

In Eq. 11 T_m is the torque generated by the motor relevant to the hull, T_f is the resisting torque due to the friction between the wheels and their axles and wall and T_s is the torque generated by motor relevant to the steering wheels.

Since the friction plays an important roll toward propulsion of the robot within the pipe, providing enough force by

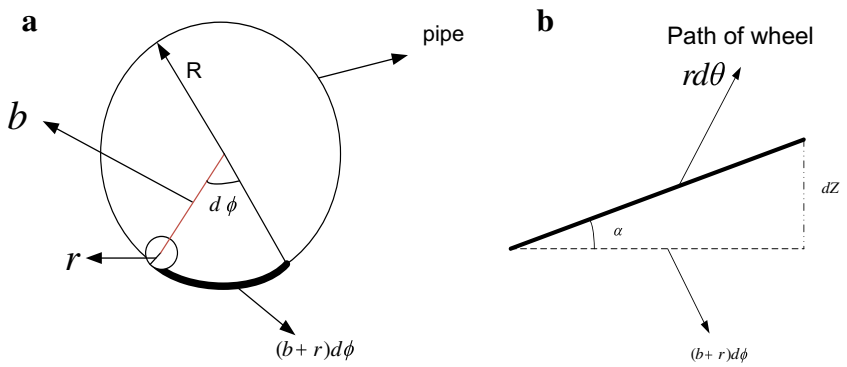

Fig. 2 **a** Frontal view of the robot in a pipe. **b** Differential element of the motion of the wheel

the axles is extremely significant in order to avoid slipping. Lack of friction at the contact point between the wheels and the pipe's wall leads to slipping the wheels which disturbs the safe and stable control of the robot. The slippage constraint of the wheel can be expressed as Eq. 12 (using Coulomb friction law):

$$f_{sn.\max} = \mu F_N \tag{12}$$

In Eq. 12 μ is the friction coefficient, F_N denotes the normal force exerted by the axles and $f_{sn.max}$ is the maximum static friction force. In the case that the system needs a friction force more than $f_{sn.max}$ in order to avoid the slippage, it is required to increase the amount of Normal force of the legs using the harder springs. So it can be shown that the required friction torque T_f is as:

$$T_f = \Gamma b \mu F_N \sin(\alpha) \tag{13}$$

where Γ is the number of active wheels.

By substituting Eq. 13 in Eq. 11 the generalized force Q_i can be computed as:

$$\begin{aligned} Q_1 &= T_m - \Gamma \mu b F_N \sin(\alpha) \\ Q_2 &= T_s \end{aligned} \tag{14}$$

Finally, by substituting Eq. 14, in Eq. 10 the dynamic differential equation of the system can be extracted as:

$$\begin{aligned} \ddot{\phi} &= \frac{\lambda R g(1+\tan^2(\alpha))\dot{\alpha} - 2R^2\alpha_M \frac{S_\alpha}{C_\alpha^3}\dot{\alpha}\dot{\phi} - \Gamma\mu b F_N S_\alpha}{\Gamma\alpha_m b^2 + I_B + R^2\alpha_M \tan^2(\alpha)} \\ &\quad + \frac{T_m}{\Gamma\alpha_m b^2 + I_B + R^2\alpha_M \tan^2(\alpha)} \end{aligned} \tag{15}$$

$$\begin{aligned} \ddot{\alpha} &= \left(\frac{R^2\alpha_M\left(\tan(\alpha)+\tan^3(\alpha)\right)}{\Gamma I_{wheel}}\right)\dot{\phi}^2 \\ &\quad - \left(\frac{\lambda R g(1+\tan^2(\alpha))}{\Gamma I_{wheel}}\right)\dot{\phi} + \frac{T_s}{\Gamma I_{wheel}} \end{aligned} \tag{16}$$

where λ is the summation of all masses and g is gravity acceleration

It can be seen that by considering the steer ability of the wheels and increasing the DOFs of the system, the number of differential equations of the system increases to two. In order to solve the mentioned coupled equations, extracting the time responses of the DOFs and finally controlling the system, it is required to rewrite the equations in the form of state space. Considering $(\emptyset.\dot{\emptyset}.\alpha.\dot{\alpha})$ as the states of the proposed inpipe robot, corresponding state space can be provided as:

$$\begin{aligned} \dot{x_1} &= x_2 \\ \dot{x_2} &= \frac{\lambda R g(1+\tan^2(x_3))x_4 - 2R^2\alpha_M \frac{S_{x_3}}{C_{x_3}^3}x_4 x_2 - \Gamma\mu b F_N S_{x_3}}{\Gamma\alpha_m b^2 + I_B + R^2\alpha_M \tan^2(x_3)} \\ &\quad + \frac{T_m}{\Gamma\alpha_m b^2 + I_B + R^2\alpha_M \tan^2(x_3)} \\ \dot{x_3} &= x_4 \\ \dot{x_4} &= \left(\frac{R^2\alpha_M\left(\tan(x_3)+\tan^3(x_3)\right)}{\Gamma I_{wheel}}\right)x_2^2 \\ &\quad - \left(\frac{\lambda R g(1+\tan^2(x_3))}{\Gamma I_{wheel}}\right)x_2 + \frac{T_s}{\Gamma I_{wheel}} \end{aligned} \tag{17}$$

3 Control Design

Two strategies are considered in this paper to control the linearized state space of the designed in pipe inspection robot and these two strategies are compared with each other. The first approach is State Vector Feedback Control (SVFC) based on Pole placement and the second one is an optimal controller according to LQR method. The first approach guaranties the dynamic response of each state according to a desired pole while the second one, controls the states in an optimal way. Both strategies are employed in this paper after in order to control the new designed in pipe inspection robot after linearization of the system about its operating point. It will be shown that this linearized optimization is applicable while its domain of attraction is large enough. So this method provides a fast and efficient closed loop optimization. In this section two mentioned controllers are designed for the in-pipe inspection screw robot with controllable wheels' angle.

3.1 Linearization Process

most of the optimal nonlinear methods of controlling strategies like Hamilton-Jacobi–Bellman are too complicated and have extremely heavy calculations which are not proper for online and real-time application of the present robot. Employing the proposed linear optimal controlling strategy of the paper not only provides an exact closed loop optimal control for the studied robot, but also is simple and fast enough which could be implemented for most of the online and real time applications with the least costs and using simple electronic boards. Similar strategy is also employed for other robotic systems [20].

As it was mentioned, for both of controlling approaches linearization of the state space is required. The linearized

state space of the designed robot about its operating point can be extracted as below:

$$\begin{aligned} \dot{X} &= AX + Bu \\ y &= CX + Du \end{aligned} \tag{18}$$

where

$$A = \frac{\partial f_i}{\partial X_j} = \begin{bmatrix} 0 & 1 & 0 & 0 \\ 0 & 0 & \frac{\Gamma F_N b\mu(0.014R^2\alpha_M - 0.99)}{0.007R^2\alpha_M + \Gamma\alpha_m b^2 + I_B} & \frac{1.007R\lambda g}{0.007R^2\alpha_M + \Gamma\alpha_m b^2 + I_B} \\ 0 & 0 & 0 & 1 \\ 0 & \frac{1.007Rg\lambda}{\Gamma I_{wheels}} & 0 & 0 \end{bmatrix} \tag{19}$$

$$B = \frac{\partial f_i}{\partial u} = \begin{bmatrix} 0 & 0 \\ \frac{1}{0.007R^2\alpha_M + \Gamma\alpha_m b^2 + I_B} & 0 \\ 0 & 0 \\ 0 & \frac{1}{\Gamma I_{wheels}} \end{bmatrix} \tag{20}$$

Considering two sensors installed on the robot to evaluate the angular position of $\emptyset$ and α, the matrixes $\boldsymbol{C}$ and $\boldsymbol{D}$ will be as:

$$C = \begin{bmatrix} 1 & 0 & 0 & 0 \\ 0 & 0 & 1 & 0 \end{bmatrix} \quad D = 0 \tag{21}$$

It will be stated in the simulation section that the linearization process is implemented about the operating point which is $([\dot{\emptyset}.\alpha.\dot{\alpha}])=([x_2,x_3,x_4])=\left([0, 5\left(\frac{\pi}{180}\right), 0]\right)$, in this paper and as it will be seen, it has a satisfying domain of attraction. As the $\emptyset = x_1$ doesn't appear in equations so the linearization is not according to the full state of the system.

3.2 Pole Placement Approach

Pole placement method is one of the classic control theories which realizes the desired performance of the states by controlling the poles of its dynamic. The system in Pole-Placement approach should be controllable [21] and it is shown in Eq. 22 that the system of this paper is controllable. Considering the Ackerman formulation, the desired characteristic equations can be defined as $\Delta_d = (s - \lambda_1)(s - \lambda_2)....(s - \lambda_n)$for which the desired poles (λ) of the system can be realized since the system is controllable as follow:

$$rank\left(\begin{bmatrix} B & AB & A^2B & A^3B \end{bmatrix}\right) = 4 \tag{22}$$

As it can be seen in Eq. 22 the rank of the controllability matrix is full (4) which shows its controllability.

According to the inputs of the system which is based on Eq. 23, the new state space will be as Eq. 24:

$$u = -K_{P-P}.X = \begin{bmatrix} K_{11} & K_{12} & K_{13} & K_{14} \\ K_{21} & K_{22} & K_{23} & K_{24} \end{bmatrix} \begin{bmatrix} \phi \\ \dot{\phi} \\ \alpha \\ \dot{\alpha} \end{bmatrix} \tag{23}$$

where $\boldsymbol{K_{P-P}}$ is the controlling gain related to Pole-Placement approach.

$$\dot{x} = Ax + Bu = (A - Bk_{p-p})x = \begin{bmatrix} \hat{A}_{11} & \hat{A}_{12} & \hat{A}_{13} & \hat{A}_{14} \\ \hat{A}_{21} & \hat{A}_{22} & \hat{A}_{23} & \hat{A}_{24} \\ \hat{A}_{31} & \hat{A}_{32} & \hat{A}_{33} & \hat{A}_{34} \\ \hat{A}_{41} & \hat{A}_{42} & \hat{A}_{43} & \hat{A}_{44} \end{bmatrix} \begin{bmatrix} \phi \\ \dot{\phi} \\ \alpha \\ \dot{\alpha} \end{bmatrix} \tag{24}$$

where

$$\hat{A}_{11} = 0 \quad \hat{A}_{12} = 1 \quad \hat{A}_{13} = 0 \quad \hat{A}_{14} = 0$$

$$\begin{aligned} \hat{A}_{21} &= -\frac{k_{11}}{0.007R^2\alpha_M + \Gamma\alpha_m b^2 + I_B}\hat{A}_{22} \\ &= -\frac{k_{12}}{0.007R^2\alpha_M + \Gamma\alpha_m b^2 + I_B} \end{aligned}$$

$$\begin{aligned} \hat{A}_{23} &= \frac{\Gamma F_N bu(0.014R^2\alpha_M - 0.99)}{0.007R^2\alpha_M + \Gamma\alpha_m b^2 + I_B} \\ &\quad -\frac{k_{13}}{0.007R^2\alpha_M + \Gamma\alpha_m b^2 + I_B} \end{aligned}$$

$$\begin{aligned} \hat{A}_{24} &= \frac{1.007R\lambda g}{0.007R^2\alpha_M + \Gamma\alpha_m b^2 + I_B} \\ &\quad -\frac{k_{14}}{0.007R^2\alpha_M + \Gamma\alpha_m b^2 + I_B} \end{aligned}$$

$$\hat{A}_{31} = 0 \qquad \hat{A}_{32} = 0 \qquad \hat{A}_{33} = 0 \qquad \hat{A}_{34} = 1$$

$$\begin{aligned} \hat{A}_{41} &= -\frac{k_{21}}{\Gamma I_{wheels}} & \hat{A}_{42} &= -\frac{k_{22}}{\Gamma I_{wheels}} - \frac{1.007Rg\lambda}{\Gamma I_{wheels}} \\ \hat{A}_{43} &= -\frac{k_{23}}{\Gamma I_{wheels}} & \hat{A}_{44} &= -\frac{k_{24}}{\Gamma I_{wheels}} \end{aligned}$$

Now for determining the feedback gain matrix ($\boldsymbol{K_{p-p}}$) of Eq. 23, the Eq. 25 should be solved and compared with the desire equation (Δ_d).

$$\left|\hat{\lambda}I - (A - BK_{P-P})\right| = \begin{vmatrix} \bar{A}_{11} & \bar{A}_{12} & \bar{A}_{13} & \bar{A}_{14} \\ \bar{A}_{21} & \bar{A}_{22} & \bar{A}_{23} & \bar{A}_{24} \\ \bar{A}_{31} & \bar{A}_{32} & \bar{A}_{33} & \bar{A}_{34} \\ \bar{A}_{41} & \bar{A}_{42} & \bar{A}_{43} & \bar{A}_{44} \end{vmatrix} \tag{25}$$

where

$$\bar{A}_{11} = \hat{\lambda} \qquad \bar{A}_{12} = -1 \qquad \bar{A}_{13} = 0 \qquad \bar{A}_{14} = 0$$

$$\bar{A}_{21} = \frac{k_{11}}{0.007R^2\alpha_M + \Gamma\alpha_m b^2 + I_B} \quad \bar{A}_{22} = \hat{\lambda} + \frac{k_{12}}{0.007R^2\alpha_M + \Gamma\alpha_m b^2 + I_B}$$

$$\bar{A}_{23} = -\frac{\Gamma F_N bu(0.014R^2\alpha_M - 0.99)}{0.007R^2\alpha_M + \Gamma\alpha_m b^2 + I_B} + \frac{k_{13}}{0.007R^2\alpha_M + \Gamma\alpha_m b^2 + I_B}$$

$$\bar{A}_{24} = -\frac{1.007R\lambda g}{0.007R^2\alpha_M + \Gamma\alpha_m b^2 + I_B} + \frac{k_{14}}{0.007R^2\alpha_M + \Gamma\alpha_m b^2 + I_B}$$

$$\bar{A}_{31} = 0 \qquad \bar{A}_{32} = 0 \qquad \bar{A}_{33} = 0 \qquad \bar{A}_{34} = \hat{\lambda} - 1$$

$$\bar{A}_{41} = \frac{k_{21}}{\Gamma I_{wheels}} \qquad \bar{A}_{42} = \frac{k_{22}}{\Gamma I_{wheels}} + \frac{1.007Rg\lambda}{\Gamma I_{wheels}}$$

$$\bar{A}_{43} = \frac{k_{23}}{\Gamma I_{wheels}} \qquad \bar{A}_{44} = \hat{\lambda} + \frac{k_{24}}{\Gamma I_{wheels}}$$

And finally the controlling input of Eq. 23 which is calculated using a local linearization, will be implemented to the original nonlinear system of the in pipe robot which results in the following closed loop state space equation:

$$\dot{x} = f(x) + g(x)u_{P-P} = \begin{Bmatrix} x_2 \\ \frac{\lambda Rg(1+\tan^2(x_3))x_4 - 2R^2\alpha_M S_{x_3} x_4 x_2 - \Gamma\mu b F_N S_{x_3}}{\Gamma\alpha_m b^2 + I_B + R^2\alpha_M \tan^2(x_3)} \\ x_4 \\ \left(\frac{R^2\alpha_M(\tan(x_3)+\tan^3(x_3))}{\Gamma I_{wheels}}\right)x_2^2 - \left(\frac{\lambda Rg(1+\tan^2(x_3))}{\Gamma I_{wheels}}\right)x_2 \end{Bmatrix} + \begin{bmatrix} 0 & 0 \\ \frac{1}{\Gamma\alpha_m b^2 + I_B + R^2\alpha_M \tan^2(x_3)} & 0 \\ 0 & 0 \\ 0 & \frac{1}{\Gamma I_{wheels}} \end{bmatrix} \times [-K_{pole-placement}.x]s \tag{26}$$

The closed loop controlling block diagram of the mentioned approach is shown in Fig. 3:

As shown in Fig. 3 the block diagram of both controllers are figured. It can be seen that based on the desired controlling approach, the strategy of controlling can be easily switched and the resultant gain can be fed to the State Feed Back Control (SVFC). Selecting the proper controller is decided by the aid of switching algorithm in an online way. In this flowchart it can be seen that, first of all, in order to tune the gains, "linear system" block is fed to the desired controller according to the mentioned switcher center. For the case in which there is no limitation on the input and just the performance of the output is important based on some desired poles, pole placement approach will be selected in which the Ackerman formula needs to be solved, while for the alternative approach of LQR, compromise will be performed between the input and accuracy and Riccati equation should be solved instead. At the same time with tuning the gains and feeding the linearized matrixes to the controllers, "Desire vector" signal is compared with "Feedback vector" and the resultant gained errors are fed to (SVFC) to be employed for calculating the required inputs based on state vector feedback controller. The calculated controlling input will be then implemented to the "plant (In-pipe inspection robot)" block finally through which the actual vector can be extracted by the sensors and be used for the feedback signal to complete the controlling loop. It should be noticed that the linearization process is based on Eqs. 19 and 20.

About the stability of the designed closed loop robot it should be considered that according to the literatures and references, closed loop systems which are controlled using LQR are always stable with a strong gain margin and phase margin [22]. Also it will be proved in the simulation section that, the domain of attraction of the closed loop system is large enough to cover an acceptable workspace of the studied robot with an acceptable accuracy. However, for the cases in which the robot is supposed to move through a long distance far from its operating point and more accuracy is expected by the robot it is possible to refresh and update the operating point of the system around which linearization is occurred. This is possible simply using the feedback signals of the sensors and a simple calculation which is extremely and significantly simpler than other nonlinear optimal controlling strategies [23].

3.3 LQR Approach

Again in this method it is supposed that all of the states are available and can be measured exactly through the sensors or observer. To solve the problem and produce the optimal input as mentioned in Eq. 27, the system should be controllable like Pole-Placement approach which is proved in Eq. 22. The controlling input of the state variable feedback regulator is the same as Eq. 23 except that the gain $\boldsymbol{K_{p-p}}$ should be replaced by $\boldsymbol{K_{LQR}}$, which its calculations is explained as below. Thus the input is:

$$u = -K_{LQR}.X \tag{27}$$

where $\mathbf{K_{LQR}}$ is the state feedback gain matrix which should be defined using LQR approach.

In this method the optimization process of LQR should be implemented based on a specific objective function. Considering the fact that accuracy and energy consumption are contradictory, the objective function is considered as below to

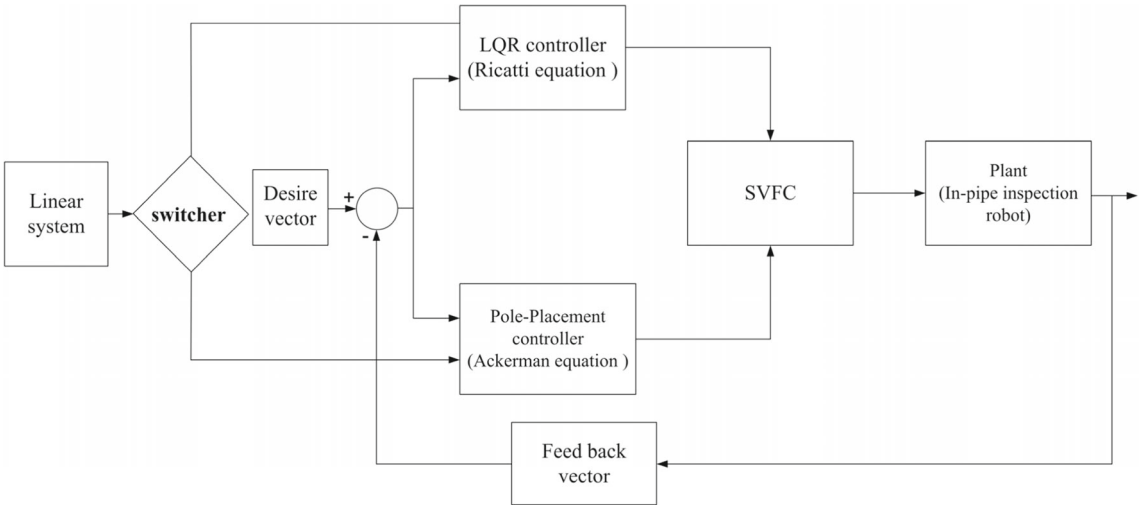

Fig. 3 Block diagram of the controlling system

provide a compromise between error and input to realize the best accuracy using the least energy consumption:

$$J = \frac{1}{2}\int_0^\infty \left(X^T Q X + u^T R u\right) dt = \int_0^\infty \left(\begin{bmatrix} x_1 & x_2 & x_3 & x_4 \end{bmatrix} Q \begin{bmatrix} x_1 \\ x_2 \\ x_3 \\ x_4 \end{bmatrix} + \begin{bmatrix} T_m & T_s \end{bmatrix} R \begin{bmatrix} T_m \\ T_s \end{bmatrix} \right) dt \tag{28}$$

where $\boldsymbol{Q}$ and $\boldsymbol{R}$, are positive definite weighting matrixes. It can be shown that the optimal controlling gain by which the mentioned objective function can be minimized should be calculated as follow:

$$K = R^{-1} B^T S = \begin{bmatrix} R_{11} & 0 \\ 0 & R_{22} \end{bmatrix} \begin{bmatrix} 0 & \frac{1}{\Gamma\alpha_m b^2 + I_B + 0.007R^2\alpha_m} & 0 & 0 \\ 0 & 0 & 0 & \frac{1}{\Gamma I_{wheels}} \end{bmatrix} s \tag{29}$$

where $\boldsymbol{S}$ can be obtained by solving the following Riccati equation.

$$\begin{aligned} A^T S + SA + Q - SBR^{-1}B^T S = {} & \begin{bmatrix} 0 & 0 & 0 & 0 \\ 1 & 0 & 0 & \frac{1.007Rg\lambda}{\Gamma I_{wheels}} \\ 0 & \frac{\Gamma F_N bu(0.014R^2\alpha_M - 0.99)}{0.007R^2\alpha_M + \Gamma\alpha_m b^2 + I_B} & 0 & 0 \\ 0 & \frac{1.007R\lambda g}{0.007R^2\alpha_M + \Gamma\alpha_m b^2 + I_B} & 1 & 0 \end{bmatrix} s \\ & + s \begin{bmatrix} 0 & 1 & 0 & 0 \\ 0 & 0 & \frac{\Gamma F_N bu(0.014R^2\alpha_M - 0.99)}{0.007R^2\alpha_M + \Gamma\alpha_m b^2 + I_B} & \frac{1.007R\lambda g}{0.007R^2\alpha_M + \Gamma\alpha_m b^2 + I_B} \\ 0 & 0 & 0 & 1 \\ 0 & \frac{1.007Rg\lambda}{\Gamma I_{wheels}} & 0 & 0 \end{bmatrix} + Q \\ & - s \begin{bmatrix} 0 & 0 \\ \frac{1}{0.007R^2\alpha_M + \Gamma\alpha_m b^2 + I_B} & 0 \\ 0 & 0 \\ 0 & \frac{1}{\Gamma I_{wheels}} \end{bmatrix} R^{-1} \begin{bmatrix} 0 & \frac{1}{\Gamma\alpha_m b^2 + I_B + 0.007R^2\alpha_m} & 0 & 0 \\ 0 & 0 & 0 & \frac{1}{\Gamma I_{wheels}} \end{bmatrix} s \end{aligned} \tag{30}$$

And consequently the closed loop linearized state space will be similar to Eq. 24 in which the gain $\boldsymbol{K_{p-p}}$ is substituted by $\boldsymbol{K_{LQR}}$:

$$\dot{x} = Ax + Bu = (A - BK_{LQR})x \tag{31}$$

The controlling block diagram of the mentioned method is also similar to Fig. 3 in which the controlling gain $\boldsymbol{K}$ is substituted by the aid of Eq. 29 and the mentioned calculations.

4 Simulation Results

Two scenarios are studied in this section. In the first scenario the performance of the ordinary previous screw in pipe

robots are compared with the new design of the steerable proposed in-pipe robot in order to show the advantage of the proposed mechanism to increase the maneuverability of the robot especially during the obstacle avoidance. In the second scenario two mentioned controlling strategies of pole placement and LQR are compared to show the superiority of LQR toward optimal controlling of the system. The main characteristics of the studied screw based in pipe robot in this paper and its related pipe specifications are mentioned in Table 2.

As it was mentioned the first step of designing the controller and implementing the LQR and Pole-Placement approaches, is linearizing the system about its operating point (linier controlling input with non-linear system), so according to Eqs. 18 and 19 the linearized system will be:

$$\begin{aligned} \dot{X} &= AX + Bu \\ y &= CX + Du \end{aligned} \tag{32}$$

where for the robot with the characteristics of Table 1 we have:

$$A = \begin{bmatrix} 0 & 1 & 0 & 0 \\ 0 & 0 & -94.78 & 673.05 \\ 0 & 0 & 0 & 1 \\ 0 & -0.0002 & 0 & 0 \end{bmatrix} \quad B = \begin{bmatrix} 0 & 0 \\ 113.6 & 0 \\ 0 & 0 \\ 0 & 3333 \end{bmatrix}$$
$$C = \begin{bmatrix} 1 & 0 & 0 & 0 \\ 0 & 0 & 1 & 0 \end{bmatrix} \quad D = 0 \tag{33}$$

4.1 Pole- Placement Approach

In order to employ the Pole-Placement approach, it is first required to define the desired poles of the system as $\boldsymbol{P}$ (Eq. 34) which provides a desired and stable response:

$$P = \begin{bmatrix} -50 & -49 & -182 & -10 \end{bmatrix} \tag{34}$$

These poles are real and negative to provide an over damped response for the states of the system. Thus the matrix $K_{\mathbf{Pole-Placement}}$ will be:

$$K_{pole-placement} = \begin{bmatrix} 18.660 & 0.066 & -21.909 & 5.714 \\ -0.718 & -0.007 & 14.964 & 0.179 \end{bmatrix} \tag{35}$$

According to the above controlling gains, the linear inputs of the Pole-Placement according to Eq. 23 will be as:

$$u_{Pole-placement} = -\begin{bmatrix} 18.660 & 0.066 & -21.909 & 5.714 \\ -0.718 & -0.007 & 14.964 & 0.179 \end{bmatrix} \times \begin{Bmatrix} x_1 \\ x_2 \\ x_3 \\ x_4 \end{Bmatrix} \tag{36}$$

4.2 LQR Approach

The same procedure is performed for LQR approach. According to Eq. 29 the matrix $\boldsymbol{K_{LQR}}$ will be as:

$$K_{LQR} = \begin{bmatrix} 2.261 & 0.018 & -10.609 & 0.006 \\ 3.08 & 0.018 & 0.717 & 0.088 \end{bmatrix} \tag{37}$$

The controller is designed aiming to stabilize and track the reference input, so the martices $\boldsymbol{Q}$ and $\boldsymbol{R}$, are chosen as:

$$Q = C^T C = \begin{bmatrix} 1 & 0 & 0 & 0 \\ 0 & 0 & 0 & 0 \\ 0 & 0 & 1 & 0 \\ 0 & 0 & 0 & 0 \end{bmatrix} \quad R = \begin{bmatrix} 0.1 & 0 \\ 0 & 0.01 \end{bmatrix} \tag{38}$$

Table 1 The value of the physical parameters of the system

Physical properties of the system			
Symbol	Value	Definition	Unit
M	0.01	Wheel mass	Kg
M_h	1	Hull mass	Kg
M_m	1	Motor mass	Kg
R	0.02	Wheel radius	m
b	0.1	Leg length	m
A	0.01	Robot's Effective Cross Sectional Area	m^2
F_N	15	The normal force of passive spring	N
μ	0.2	Friction coefficient	–
I_B	10^{-4}	Hull polar Moment of Inertia	$Kg.m^2$
I_{WZ}, I_{WX}	10^{-8}	Wheel Moment of Inertia around the pipe axis	$Kg.m^2$
G	9.8	Gravity	$\frac{m}{s^2}$
Γ	3	Number of active wheels	
I_{wheel}	$2*10^{-8}$	Wheel Moment of Inertia around the leg	$Kg.m^2$

which consequently results in the following optimal input:

$$u_{LQR} = -\begin{bmatrix} 2.261 & 0.018 & -10.609 & 0.006 \\ 3.08 & 0.018 & 0.717 & 0.088 \end{bmatrix} \begin{Bmatrix} x_1 \\ x_2 \\ x_3 \\ x_4 \end{Bmatrix} \quad (39)$$

4.3 Kinematics and Dynamics

As it was explained, the possibility of the obstacle avoidance during the movement through the pipe is provided by the aid of the proposed robot since the angle of the wheels are controllable. Figure 4 compares the workspace movement of the ordinary robot and the robot which is equipped by variable wheels' angle. This figure shows that the proposed robot of this paper is able to by-pass an obstacle which is considered in the inner surface of the pipe by changing the angle of its wheels while the ordinary in pipe robot is collided with the mentioned obstacle.

According to Fig. 4 it can be seen that, not only the obstacle is bypassed using the proposed robot configuration, but also a faster movement is provided for the new designed robot since the pitch rate of the screw based in pipe robot is also controllable with variable wheels' angle. Since the stability of the robot is extremely dependent to the front wheel by which the steering of the robot should be handled, collision of the rear wheel with small obstacles could not be important and it could be damped using a simple suspension system. Another advantage of the proposed mechanism is providing a movement with variable speed without the necessity of changing the rotational velocity of the main joint motor.

Also the velocity of the robot center and its comparison between the ordinary system and the proposed system with variable angle can be seen in Fig. 5:

It can be seen that the velocity of the robot with variable angle can be increased according to its related controlling command while the velocity is constant for the system with fixed wheels' angle. Also, because the studied robot in this paper travels in a straightforward pipe, its velocity along the X and Y directions are zero and the main projection of its velocity is along the Z axis.

The kinematic results of the joint space of the robot and its comparison between the simple system and the new proposed system can be observed in Fig. 6.

Figure 5 shows that however the angular velocity of the first joint space which is related to the main screw rate of the rotational part of the robot is roughly the same for both systems, but the third state (α) of the joint space of the robot can be independently controlled for the proposed system. As a results this state which is related to the wheels' angle is constantly zero for the simple system while this angle is monotonically increasing in the proposed controllable angle system to by-pass the obstacle.

As mentioned above the system is steerable so, in Fig. 6 the comparison of the first and second states ($\dot{\emptyset}\dot{\emptyset}$) can be observed between the fixed and variable wheels' angle systems. It is noticeable that the system with variable angle is considerably more compatible and flexible with tracking the desired path with higher accuracy.

And finally Fig. 6 shows the response of the fourth state ($\dot{\alpha}$). Since the angle is constant for the fixed angle system, its derivative is also zero as expected while this state experiences a short oscillatory behavior before its settling time as a result of the nature of SVFC controller.

The inputs of the systems and their comparison between variable and fixed angle systems are shown in Fig. 7. It's obvious from the Fig. 7 that the system with fixed angle just needs one input while in the proposed model of variable angle, two controlling input is required to control the rotational angle of the main body and the angle of the

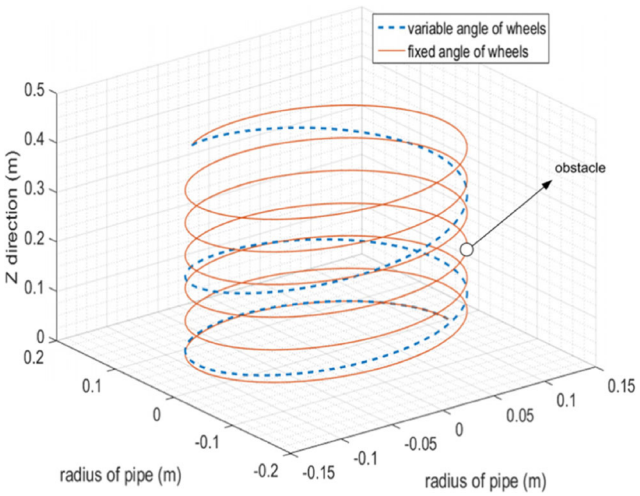

Fig. 4 Passing the obstacle by controlling the angle of the wheels

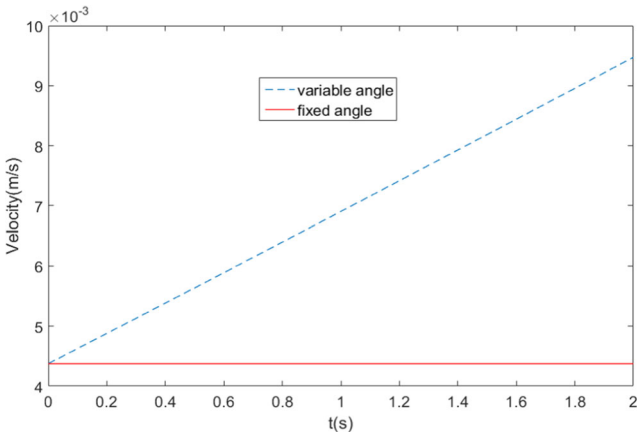

Fig. 5 The Z direction velocity of the robot center through the pipe

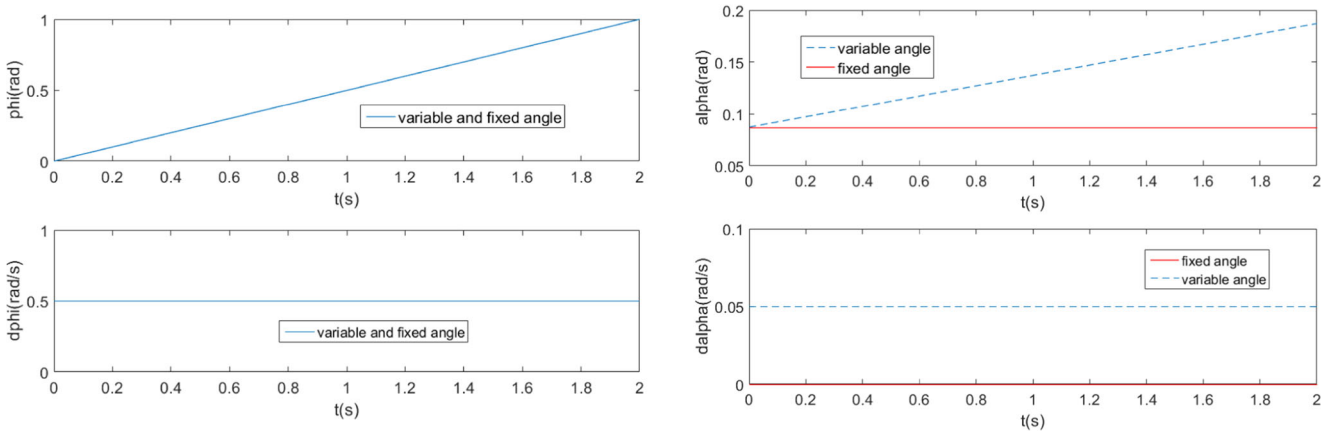

Fig. 6 Responses of the joint space parameters

wheels simultaneously. Considering the fact that the translational movement of the robot with variable wheels' angle can be accelerated by the aid of its steering control, the required torque of the robot with variable wheels' angle is considerably lower for a same displacement.

4.4 Control Results

As mentioned above, two types of controllers including of LQR and Pole Placement are designed and examined in order to track the robot along its desired path. In this section both of the mentioned approaches are employed for a same scenario in order to show the superiority of LQR toward optimization of the system. The plant of both cases is the new proposed in-pipe inspection robot with controllable wheels' angle.

The employed control parameters of the system for both approaches are mentioned in Table 2.

As shown in Fig. 8 the desired path of the robot with variable angle is a cylindrical path with variable pitch rate and can be controlled according to Eq. 40:

$$Z = R\emptyset tan(\alpha) \tag{40}$$

In order to compare the responses of the states using two mentioned controlling approaches, a ramp input is considered as the desired input and so the desired state inputs of x_1 and x_3 can be stated as a function of time with slopes of 0.05 and 0.005 respectively. Thus, the equations of the desired inputs are:

$$x_1 = 0.05t \tag{41}$$

$$x_3 = 0.005t \tag{42}$$

According to the controlling gains and the specifications of Table 2 and Section 3 the actual path of the robot for both cases are obtained as Fig. 8.

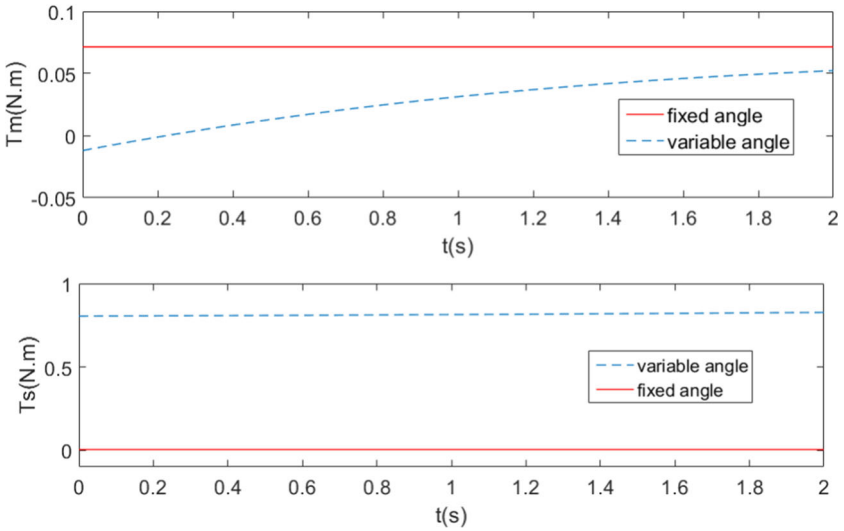

Fig. 7 Comparison of the inputs for variable and fixed angle system

Table 2 The control parameters

Definition	value
Desire Poles of Pole-placement	$[\emptyset.\dot{\emptyset}.\alpha.\dot{\alpha}]=[-50\ ,-49\ ,-182\ ,-10]$
The controller gain ($K_{Pole-Placement}$)	$K_1 = [8.1510\ ,-0.3989\ ,-16.7818\ ,5.6070]$
	$K_2 = [\ -0.5805\ ,-0.0121\ ,2.5804\ ,0.0668]$
The controller gain (K_{LQR})	$K_1 = [2.2618\ ,0.0180\ ,-10.6091\ ,0.0063]$
	$K_2 = [\ 3.0803\ ,0.0184\ ,0.7177\ ,0.0887]$

First of all, it can be seen that using both of controlling approaches, the desired path which is a helical way with variable pitch rate is realized thanks to steerable design of the robot. Afterwards, it can be concluded that both approaches have provided an acceptable accuracy since the controlling gains are properly adjusted. However, it can be seen that the LQR approach provides a faster tracking rather than Pole-Placement, since the desired movement is realized in this method during the finite simulation time but the movement of the robot for the case in which the system is controlled using pole placement approach is incomplete during the mentioned time.

Each states of the robot and its comparison for two controlling approaches can be seen as below:

Figure 9 indicate that the LQR controller has a better response while not only the accuracy is slightly better, but also its vibrating response at the first stages of the simulation is less. By the other word, LQR has provided slightly over damped responses since the responses of pole placement approach is almost under damped. It should be noticed here that the response of the pole placement is underdamped despite of real negative poles which are considered as the desired poles of the system. This phenomenon is contributed to the fact that the controlling input of the linearized controller is implemented on the real nonlinear system. However, it can be seen that despite of the fact that both of LQR and pole placement approaches are linear controllers, but the response of LQR is more biased to over damped response as a result of its proper error optimization. Also as it will be seen later, the domain of attraction of the system through which the employed linearization is valid is sufficiently wide which shows the applicability of this optimum controller for this nonlinear system.

Figure 10 shows the domain of attraction of each controlling approach. The linearization point should be specified according to operating point about which the robot is expected to operate within mostly. It should be considered that the original nonlinear system is linearized here about $([0,5(\frac{\pi}{180}),0])$ and the employed linear controller has an effective domain of attraction in where the controller is able to realize the tracking successfully. It is proved in Fig. 10, that the domain of attraction is sufficiently large which can cover an acceptable workspace for the robot. However, the mentioned operating point can be refreshed in some specific time intervals in the cases for which the robot is supposed to move through a long distance far from its calculated domain of attraction.

The mentioned domain of attraction is compared in the above figures. It can be seen that the mentioned effective time interval of LQR is about 90sec while this value is about 161sec for the second approach. It is contributed to the fact

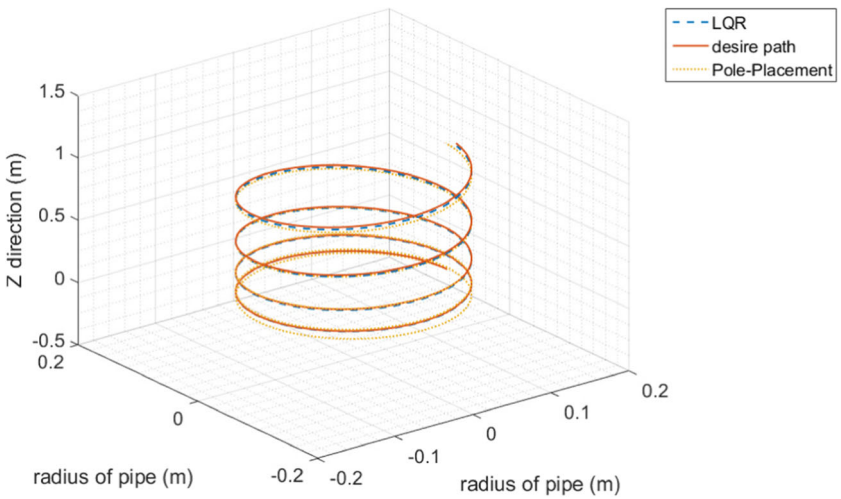

Fig. 8 Path of the robot on the inner wall of the pipe using two controlling approaches

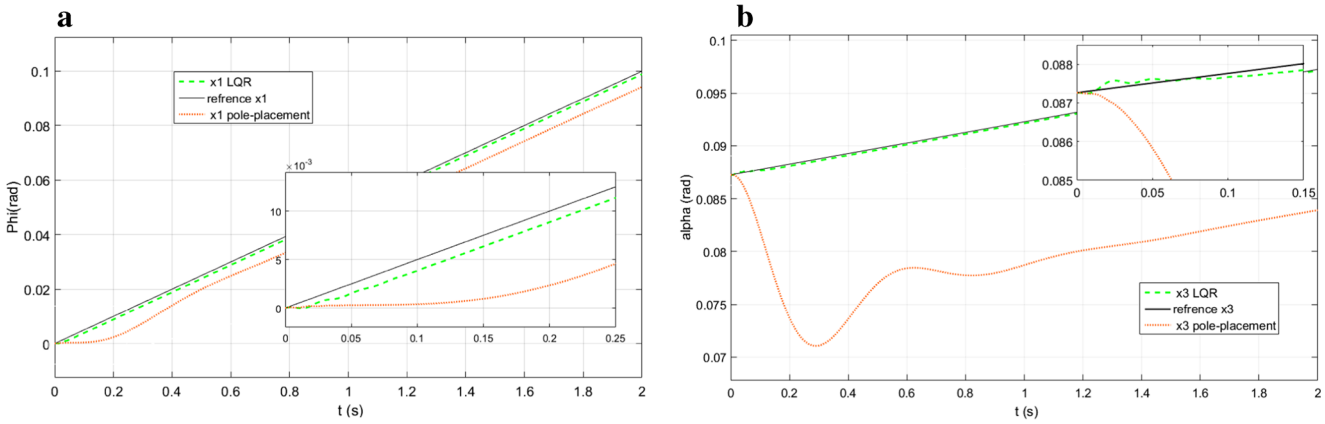

Fig. 9 **a** Response of x_1 (ϕ) **b** Response of x_3 (α)

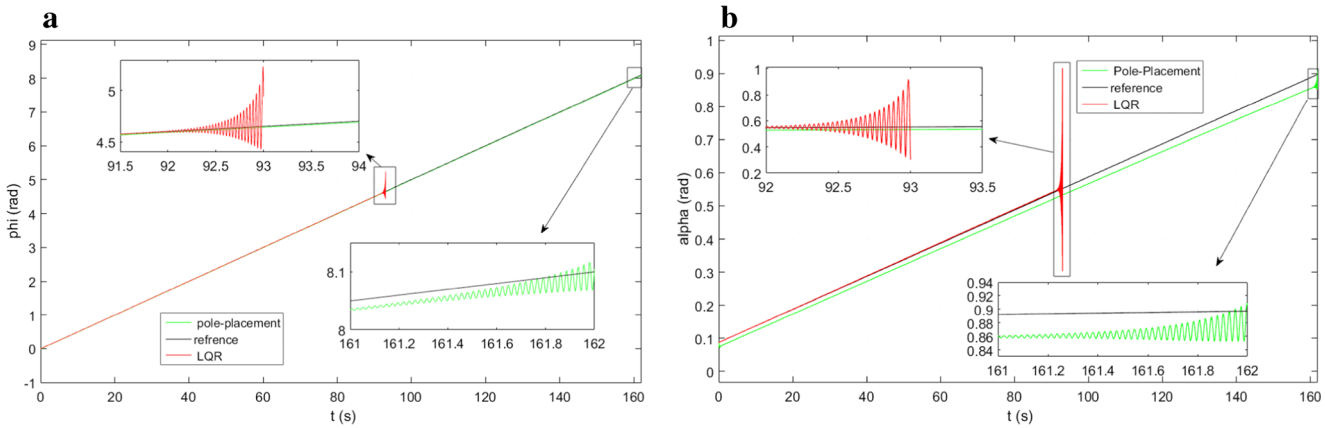

Fig. 10 **a** Domain of attraction of first state ($\emptyset$) **b** Domain of attraction of third

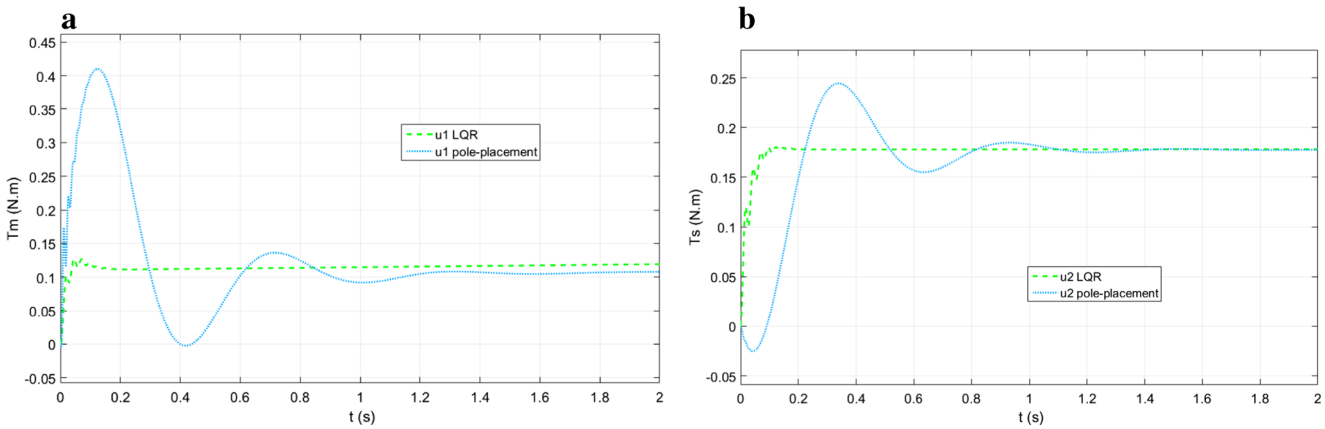

Fig. 11 **a** Comparison of first input (T_m) **b** Comparison of second input (Ts)

that the imaginary part of the poles related to LQR are not zero while the poles related to the desired poles of the pole placement approach are selected purely real. This imaginary part causes a harmonic response with higher frequency in X. Considering the fact that the employed controlling strategies for both cases of LQR and Pole-Placement are state vector feedback and thus the input is a function of the states, U=-KX, it can be concluded that according to Eq. 26 the nonlinear functions of $f(x)$ and $g(x)$ which are functions of X will be also harmonic. This fact causes increasing the error of truncation of Tylor series through linearization approximation of the model since the higher order of the series are also nonlinear harmonic functions and thus are not zero and could not be eliminated. Since the frequency in the LQR is nonzero, the error of eliminating the mentioned items in the Tylor series increases respect to pole placement and cases decreasing the domain of attraction of the system controlled by LQR:

$$\left.\begin{array}{l} P_{P.P} = \left[\,-50\ \ -49\ \ -182\ \ -10\,\right] \\ P_{LQR} = \text{[-2.02 -1.03+1.57i -1.03-1.57i -0.016]} \end{array}\right\} \rightarrow \left\{\begin{array}{l} \omega_{P.P} \approx 0 \\ \omega_{P.P} \approx 1.57 \end{array}\right. \qquad (43)$$
$$\frac{\partial^n f}{\partial x^n}(LQR) >> \frac{\partial^n f}{\partial x^n}(P.P); \quad n > 1$$

So the domain of attraction of the system can be estimated about 3meters for LQR and about 7meters for pole placement which are large enough to ensure the applicability of linearizing process and is achieved by LQR faster that pol placement.

Now in order to demonstrate the optimality of LQR and comparing its energy consumption respect to pole placement approach, the kinetic results of controlling inputs are extracted which can be seen as follow:

Again here Fig. 11 indicate that, not only the net value of inputs of LQR controller is less than pole placement, but also its semi-over damped response shows its superiority respect to pole placement toward controlling a nonlinear system like in-pipe robot.

As mentioned in Eq. 28 the LQR is designed with the aim of providing the optimality of the objective function, so the objective function is calculated here during the simulation to compare this cost function between these two approaches.

$$J_{LQR} = \frac{1}{2}\int_0^\infty \left(X^T Q X + u^T R u\right) dt = \int_0^\infty \left(\left[\, x_1\ x_2\ x_3\ x_4 \,\right] Q \begin{bmatrix} x_1 \\ x_2 \\ x_3 \\ x_4 \end{bmatrix} + \left[\, T_m\ T_s \,\right] R \begin{bmatrix} T_m \\ T_s \end{bmatrix} \right) dt = 158246446.80 \qquad (44)$$

$$J_{Pole-Placement} = \frac{1}{2}\int_0^\infty \left(X^T Q X + u^T R u\right) dt = \int_0^\infty \left(\left[\, x_1\ x_2\ x_3\ x_4 \,\right] Q \begin{bmatrix} x_1 \\ x_2 \\ x_3 \\ x_4 \end{bmatrix} + \left[\, T_m\ T_s \,\right] R \begin{bmatrix} T_m \\ T_s \end{bmatrix} \right) dt = 3999219787.46 \qquad (45)$$

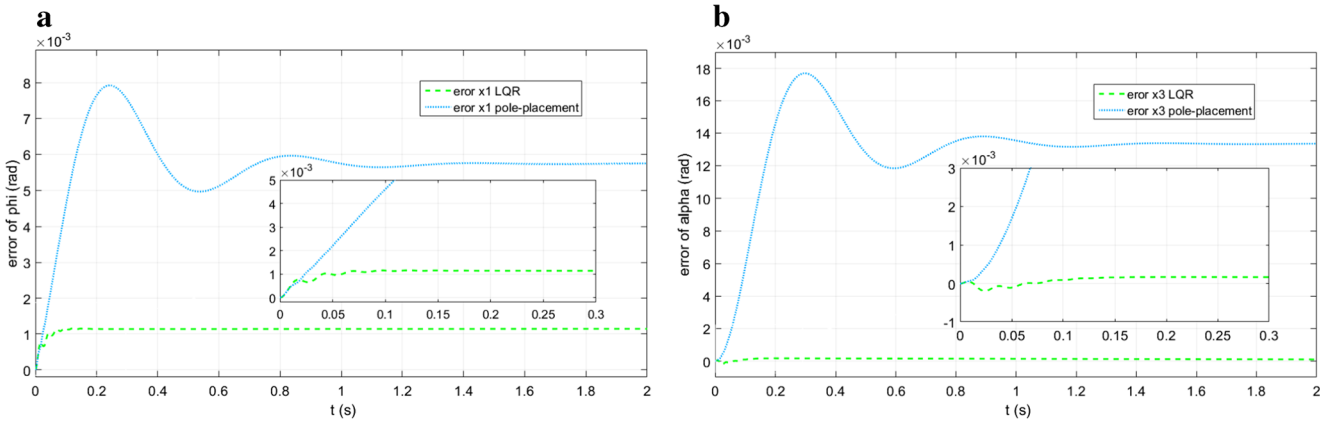

Fig. 12 **a** Error of first state (φ) **b** Error of second state (α)

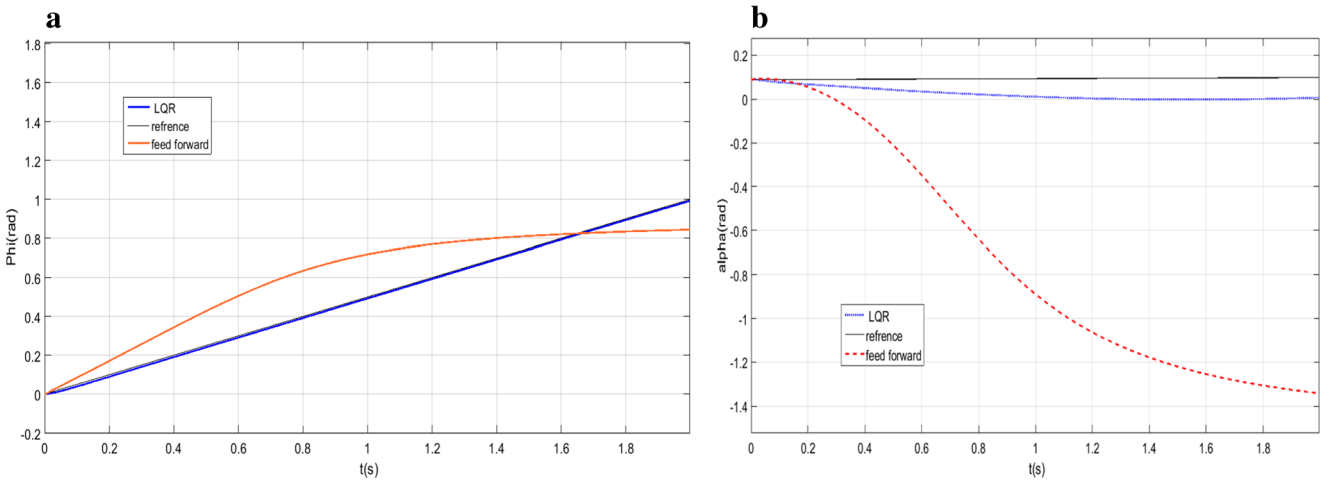

Fig. 13 **a** response of x1 **b** response of x_3

So it is obvious in Eqs. 44 and 45 that the objective function in LQR approach is considerably less as it was expected which verifies the optimality of this approach and its superiority in minimizing the error and energy.

Also the states' error of the controllers during the tracking of the robot is compared for two cases in the following figure:

It is obvious from Fig. 12 that despite of the acceptable accuracy of both controllers which is of order10^{-3}, but again the integral of tracking error during the simulation is considerably decreased for the system which is controlled by the aid of LQR

In order to show the robustness of LQR approach, in Fig. 13, there is a comparison between LQR and feedforward control method for tracking a desired path of $((x_{1d} = 0 \bullet 5t$ and $x_{3d} = 0 \bullet 005t + (5\pi/180)))$ in presence of disturbance of *sin(t)*.

It is obvious that LQR controller tracks the desired path accurately, while in the feedforward approach significant deviation can be observed which shows the robustness of the proposed controlling algorithm compared to traditional computed torque method

5 Verification

In order to verify the validity of MATLAB results and prove the efficiency of the proposed in-pipe robot, the proposed system is modeled in ADAMS and the related kinematic and kinetic results are compared with MATLAB. Figure 14 shows the modeled screw based in-pipe robot in ADAMS.

The black section in the figure is related to the stator part of the robot while the red one shows the rotor of the system Also, in Table 3 ADAMS simulation details are shown to depict the designed parameters of simulation

As mentioned about steerability of the proposed robot in this paper, the new designed model of the steer mechanism together with related gears is shown in Fig. 14 It can be seen that the second motor with bevel gears can change the angle of wheels (Fig. 15).

In Sections 3–4, both of kinematic result of joint space and work space and also their related kinetic responses were figured. Here the mentioned results are derived again in ADAMS to check the validity of the simulation Fig. 16 compares the workspace output of kinematic results between

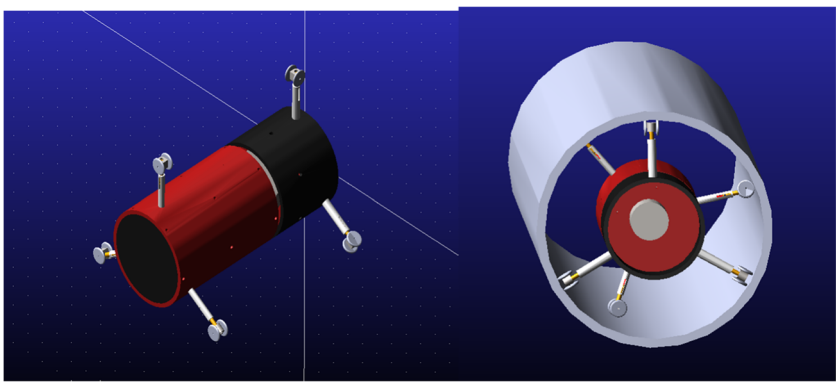

Fig. 14 Model of the proposed in-pipe robot in ADAMS

Table 3 Parameters in ADAMS

Definition	Value
Coulomb friction	On
Static coefficient	0.3
Dynamic coefficient	0.2
Stiction Transition	0.1
Friction Transition	1

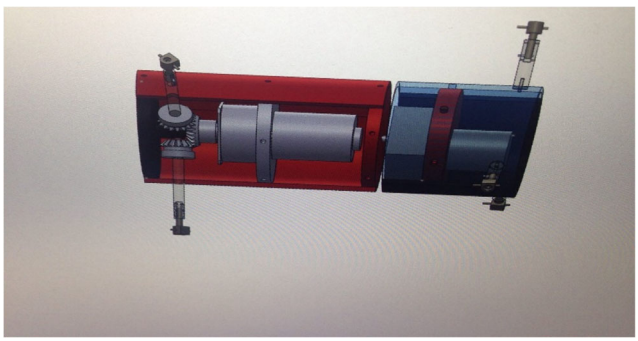

Fig. 15 Designed steer mechanism of the robot

MATLAB and ADAMS for the joint space input of Fig. 6 with variable wheels' angle.

Comparison of position and velocity of the robot workspace output shows the good compatibility of the results between MATLAB and ADAMS. This good compatibility of the response trends proves the correctness of modeling and simulating the robot in MATLAB. The small deviation and slope difference in the response of the ADAMS profile respect to MATLAB is related to the parametric uncertainties like flexibility of the legs, frictional condition and etc. which are modeled in ADAMS and are ignored in MATLAB simulations.

6 Conclusion

A new mechanism of in-pipe inspection robot was designed and controlled in this paper based on screw movement which is steerable and its wheels' angle are controllable. All of the related kinematics and kinetics formulation of the proposed robot were derived. Afterward, the robot was controlled using two strategies of pole placement and LQR. The superiority of the new proposed in pipe robot respect to previous ordinary types was shown by the aid of a comparative simulation study. It was seen that the proposed steerable robot has a better maneuverability and especially it is able to successfully by-pass a predefined obstacle by controlling its wheels' angle and its pitch rate. Also it was seen that this feature can provide a movement of the robot with controllable pitch rate which results in variable speed movement of the robot without changing the motor speed of the main rotational joint of the robot.

Afterwards two kinds of controllers were designed and implemented on the robot including pole placement and LQR. It was seen that however the accuracy of both controllers are acceptable and their errors are of order 10^{-3} but

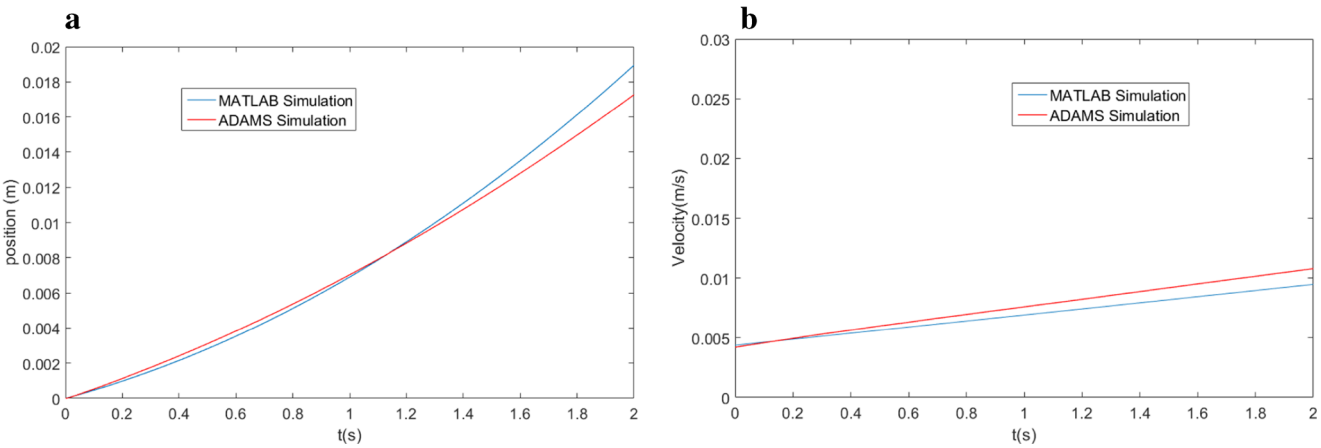

Fig. 16 **a** the comparison of center position. **b** the comparison of center velocity

closed loop optimal controller of LQR can offer more benefits for our plant. It was shown that using LQR approach not only provides an optimal closed loop controlling system by which higher accuracy and faster response can be achieved using less power, but also its compatibility with nonlinear systems is considerably better since it can control the states with semi- over damped response with a significantly wide range of domain of attraction. Also the performance of the proposed controlling strategy was compared to simple traditional nonlinear controller of computed torque method and it again the robustness and optimality superiority of the proposed controller was confirmed. Analyzing the domain of attraction of the employed controllers also showed that this range is satisfactorily wide to ensure us of applicability of this controller for the proposed nonlinear in pipe robot. Thus the efficiency of the designed robot and also controller were verified using analytic simulations and it was proved that a considerable improvement can be implemented on the screw based in pipe robots using the mentioned proposed structure while all of the states' response can be successfully controlled by the aid of the proposed optimal controller to realize the robot trajectory with the best accuracy and the least power consumption. At the end the validity of all of the kinematic and kinetic result were verified by modeling the proposed robot in ADAMS and comparing the results. The acceptable compatibility of the program files proved the correctness of modeling and simulating the robot.

References

1. Peng, Z., Yang, S., Wen, G., Rahmani, A., Yu, Y.: Adaptive Distributed Formation Control for Multiple non-Holonomic wheeled mobile robots. Neurocomputing **173**, 1485–1494 (2015)
2. Scaglia, G., Serrano, E., Rosales, A., Albertos, P.: Linear interpolation based controller design for trajectory tracking under uncertainties: application to mobile robots . Control. Eng. Pract. **45**, 123–132 (2015)
3. Takahashi, M., Hayashi, I., Iwatsuki, N., Suzumori, K.: The Development of an In-Pipe Micro robot Applying the Motion of an Earthworm, Micro Machine and Human Science (1994)
4. Zagler, A., Pfeiffer, F.: (MORITZ) A Pipe Crawler for Tube Junctions. Robot. Autom. **3**, 2954–2959 (2003)
5. Kim, J.H., Sharma, G., Iyengar, S.S.: FAMPER: A Fully Autonomous Mobile Robot for Pipeline Exploration, Industrial Technology (ICIT), pp. 517–523 (2010)
6. Harish, P., Venkateswarlu, V.: Design and Motion Planning of Indoor Pipeline Inspection Robot, International Journal of Innovative Technology and Exploring Engineering (IJITEE), vol. 3 (2013)
7. Suzumori, K., Miyagawa, T., Kimura, M., Hasegawa, Y.: Micro Inspection Robot for 1-in Pipes. Mechatronics **4**, 286–292 (1999)
8. Zhang, Y., Yan, G.: In-pipe Inspection Robot With Active Pipe-Diameter Adaptability and Automatic Tractive Force Adjusting. Mech. Mach. Theory **42**, 1618–1631 (2007)
9. Roh, S., Choi, H.R.: Differential-Drive In-Pipe Robot for Moving Inside Urban Gas Pipelines. Robotics **21**, 1–17 (2005)
10. Nayak, A., Pradhan, S.K.: Design of a New In-Pipe Inspection Robot. Procedia Eng. **97**, 2081–2091 (2014)
11. Li, P., Ma, S., Li, B., Wang, Y.: Multifunctional Mobile Units With a Same Platform for In-Pipe Inspection Robots, Intelligent Robots and Systems, pp. 2643–2648 (2008)
12. Kakogawa, A., Ma, S.: Mobility of an In-pipe Robot With Screw Drive Mechanism Inside Curved Pipes, Robotics and Biomimetics (ROBIO), pp. 1530–1535 (2010)
13. Yanheng, Z., Mingwei, Z., Hanxu, S., Qingxuan, J.: Design and Motion Analysis of a Flexible Squirm Pipe Robot, Intelligent System Design and Engineering Application, pp. 527–531 (2010)
14. Pyrkin, A.A., Bobtsov, A.A., Kolyubin, A., Faronov, M.V., Borisov, O.I., Gromov, V.S., Vlasov, M.N., Nikolaev, A.: Simple Robust and Adaptive Tracking Control for Mobile Robots. IFAC-PapersOnLine **48**, 143–149 (2015)
15. Pitanga, J.R., Araújo, H.X., Conceição, A.G.S., Oliveira, G.H.C.: Stable Model-Based Predictive Control for Wheeled Mobile Robots using Linear Matrix Inequalities. IFAC-PapersOnLine **48**, 33–38 (2015)
16. Heidari, A.H., Mehrandezh, M., Paranjape, R., Najjaran, H.: Dynamic Analysis and Human Analogous Control of a Pipe Crawling Robot, Intelligent Robots and Systems, pp. 733–740 (2009)
17. Zhang, H., Gong, J., Jiang, Y., Xiong, G., Chen, H.: An Iterative Linear Quadratic Regulator Based Trajectory Tracking Controller for Wheeled Mobile Robot. J. Zhejiang University Sci. C Comput. Elect. **13**, 593–600 (2012)
18. Lang, H., Wang, Y.: Visual Servoing With LQR Control for Mobile Robot, Control and Automation (ICCA), pp. 317–321 (2010)
19. Kakogawa, A., Ma, S.: Mobility of an in-pipe robot with screw drive mechanism inside curved pipes, Robotics and Biomimetics (ROBIO), pp. 1530–1535 (2010)
20. Korayem, M.H.: Maximum DLCC of Spatial Cable Robot for a Predefined TrajectoryWithin the Workspace Using Closed Loop Optimal Control Approach. J. Intell. Robot. Syst. **63**, 75–99 (2011)
21. Chen, C.T.: Introduction to linear system theory (1984)
22. Lin, F.: Robust Control Design an Optimal Control Approach. Wayne State University, USA and Tongji University, China Copyright Research Studies Press Limited. Published by Wiley, England (2007)
23. Nikoobin, A.: Determining of Dynamic Load Carrying Capacity of Flexible Manipulators via Optimal Control, PhD Thesis, Iran University of Science and Technology (2008)

H. Tourajizadeh was born in Tehran, Iran on October 30, 1984. He received his B.Sc. in Mechanical Engineering from KNT University of Technology in 2006. He has obtained his M.Sc. from Iran University of Science and Technology in 2008 in the field of applied mechanical design. He also has obtained his Ph.D. from Iran University of Science and Technology in 2012 in the same field, branch of control and vibration. More than 20 ISI papers, 6 scientific and research papers, 13 accepted conference papers, 1 published book,1book chapter and 2 booked inventions are the results of his researches so far. He has been involved in teaching and research activities for more than 9 years in the field of control and dynamics in different universities and he is now assistant professor of Kharazmi University. His research interests include robotic systems, automotive engineering, control and optimization, parallel manipulators, industrial automation and mechatronic systems and he has supervised more than 5 M.Sc. theses so far.

M. Rezaei was born in Khomein, Iran on June 22, 1991. He received his B.Sc. in Mechanical Engineering from Damavand university in 2013. He is studying in M.Sc. in Kharazmi university in the field of applied mechanical design. Two accepted conference paper, is the results of his studying so far. He is the Secretary of the mechanics and robotics Association in Kharazmi university. His research interests include robotic systems, control and optimization, parallel manipulators, industrial automation and mechatronic systems.

A. H. Sedigh was born in Tehran, Iran on June 26, 1996. He is studying B.Sc. in Mechanical Engineering at Kharazmi university. His research interests include robotic systems, control, industrial automation and mechatronic systems.